

Quantum chemical studies on the mechanistic aspects of tandem sequential cycloaddition reactions of cyclooctatetraene with ester and nitrones

Ernest Opoku, Richard Tia*, Evans Adei

Theoretical and Computational Chemistry Laboratory, Department of Chemistry, Kwame Nkrumah University of Science and Technology, Kumasi, Ghana

ARTICLE INFO

Article history:

Received 18 April 2019

Received in revised form

26 June 2019

Accepted 27 June 2019

Available online 5 July 2019

Keywords:

Isoxazolidines

Mechanistic study

Tandem addition

Cyclooctatetraene

Nitrones

ABSTRACT

The mechanisms of the tandem sequential $[4 + 2]/[3 + 2]$ and $[3 + 2]/[4 + 2]$ cycloaddition sequences involving an ester, cyclooctatetraene (COTE), and cyclic and acyclic nitrones for the formation of a diverse range of isoxazolidine derivatives and other synthetic precursors are reported. A thorough exploration of the PES has characterized several regio-, stereo- and enantio-selective mechanistic channels involved in these reactions. A perturbation molecular orbital (PMO) analysis been employed to rationalize the results. It has also been found that the initial electrocyclic ring closure of the COTE is the rate-determining step in the tandem sequential $[4 + 2]/[3 + 2]$ addition sequence. The thermolytic breakdown of the tandem adducts to subsequent monocyclic, bicyclic and tricyclic adducts occurs generally with very high activation barriers making it an inconvenient synthetic approach. The different reactivity of all the three double bonds present in the dipolarophile is reported. Finally, the mechanistic possibilities of $[3 + 2]/[4 + 2]$ addition sequences involving the same reaction components in the case of cyclic and acyclic nitrones are explored extensively. The results suggest a novel and convenient routes for obtaining products of high selectivity with less energetic requirements. In some instances, new cycloadducts hitherto unreported are obtained.

© 2019 Elsevier Inc. All rights reserved.

1. Introduction

Current trends in synthetic organic chemistry requires the ability to carry out multiple chemical transformations in a single step conveniently. Such approaches enhance synthetic efficiency, hence its widespread recognition. Synthetic methods that meet this objective are deemed extra ordinary especially when there is no need for isolation of intermediates or a change in reaction conditions until the expected product is obtained [1].

In the domain of organic reactions, cycloaddition has become a powerful synthetic tool employed in the rapid construction of complex molecules (natural products) from simpler and cheaper analogues. The extensive recognition offered to cycloaddition reactions is due to mostly its flexibility and ability to form various bonds, rings, and stereocenters in a single chemical transformation, which is crucial for enhanced synthetic efficiency [2–7].

Under the umbrella of cycloaddition reactions is tandem addition reactions which is sometimes referred as one pot synthesis. Tandem addition reaction is a method in the synthetic tool kit which allows for successive reactions in a single pot without the need to isolate intermediates until the final product(s) is/are formed. The usefulness of this method is the suitability it affords in synthesizing compounds without the need for complex apparatus and expensive reagents to isolate intermediates for subsequent reactions [1,3,4].

Tandem cycloaddition reactions have been categorized [1] into three, comprising tandem cascade, consecutive, and sequential cycloadditions reactions respectively. Tandem cascade (domino) refers to reactions in which all reactants and reagents required are incorporated from the onset of the reaction. No further additions or changes are made to such reactions until the expected adducts are obtained. Reactions in which two reactive components are made to react, usually under thermal conditions, to generate an adduct of required functionalities followed by addition of a third reactive component and change in reaction conditions (usually to photochemical) to form a tandem adduct are categorized as tandem consecutive addition reactions. In tandem sequential

* Corresponding author.

E-mail addresses: ernopoku@gmail.com (E. Opoku), richardtia.cos@knust.edu.gh, richtiagh@yahoo.com (R. Tia), eadei@yahoo.com (E. Adei).

cycloadditions, two reactive components are employed at the beginning of the reaction to form an intermediate of required functionalities. A third reactive component is then introduced to react with the intermediate to yield the final tandem adduct. It should be noted that no change in reaction conditions is required and isolation of the intermediate is not a necessity [2,8].

Danishefsky and co-workers have made use of tandem sequential cycloaddition reactions for the syntheses of natural products (vernolepin and vernomenin) in earlier reports [9]. Recently, Sears and his team [3,10] has employed this synthetic approach to synthesize vindolein. Several reports are available in the literature wherein tandem sequential cycloaddition strategy has been utilized for diverse synthetic applications [11–15].

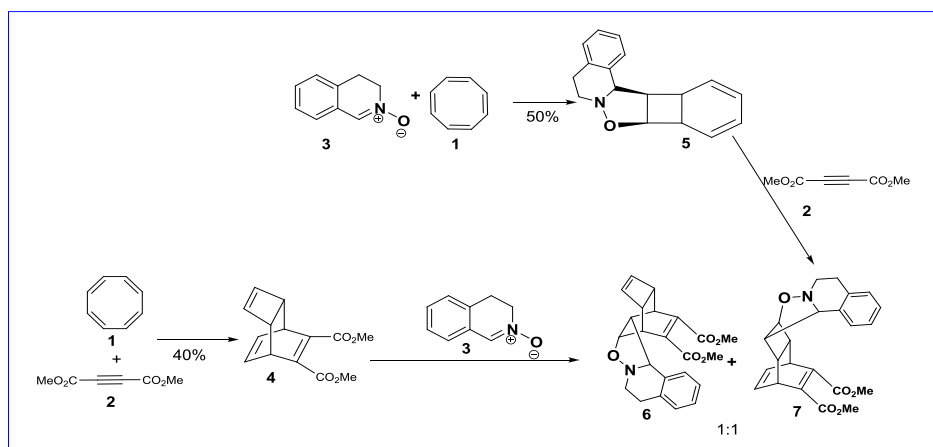
Bianchi and his co-workers have reported a fascinating tandem sequential $[4 + 2]/[3 + 2]$ cycloaddition involving the use of cyclooctatetraene (COTE), alkynes and selected 1,3-dipoles [16,17]. Reaction of COTE (**1**) with dimethyl acetylenedicarboxylate (**2**) yields an unusual tricyclic product (**4**) that arises from an initial $[4 + 2]$ cycloaddition (Scheme 1). Subsequent reaction of **4** with 3,4-dihydroisoquinoline N-oxide (**3**) [16] affords a mixture of tandem cycloadducts **6** and **7** in equal yields as shown in Scheme 1. However, when **1** and **3** are employed as the starting materials, a $[3 + 2]$ adduct **5** was obtained in 50% yield. Follow up addition of **5** with **2** leads to a regioselective adduct **7**. However, no attempt was made to explore the possibility of an initial addition of the **2** and **3** for adduct formation and a subsequent reaction with the COTE to ascertain how that route may affect product outcomes. Bianchi and his team [16] noted that this synthetic approach may serve as a general entry for obtaining new interesting cyclobutane-condensed heterocyclic systems, especially isoxazolidines derivatives. Hence, they extended their study by employing acyclic nitrones as the dipoles (Scheme 2). In this instance, an initial cycloaddition of COTE with the acyclic nitrones was found to be more sluggish and no definite product was successfully isolated. However, reaction of **8** with Diels Alder adduct **4** led to the formation of tricyclic tandem adducts **9**, **10** and **11**. It should be noted that structure **11** is tentative as its stereochemistry was not conclusively determined. Thermolytic breakdown of diastereomeric adduct **9** and **10** lead to formation of dimethyl phthalate **13** and diastereomeric 3-methyl-4-phenyl-2,3-oxazabicyclo[3.2.0]hept-6-enes **12** and **14** in 36% overall. In an ensuing study, Bianchi et al. [17] employed nitrile imines as the dipole with the tricyclic diester adduct.

The popularity of tandem sequential $[4 + 2]/[3 + 2]$ of any sequence/order is credited to Denmark and his co-workers [1,8,15,18] who have employed this strategy to construct

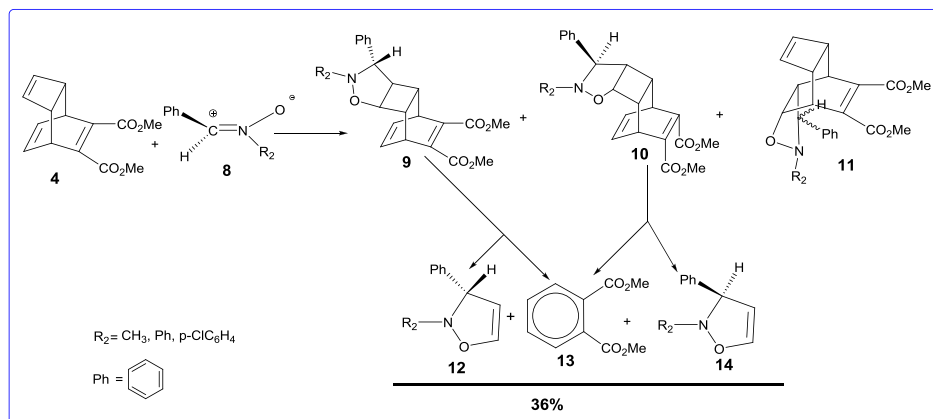
countless heterocyclic structures. The works of Bianchi et al. [16,17] affords a convenient route to obtain various derivatives of isoxazolidines and pyrazolines. Due to the potentials of isoxazolidines as biologically-relevant precursors [19,20] and their application in environmental remediation [21], several attempts are ongoing in synthesizing various derivatives [22–28]. A thorough search of the chemical literature revealed that comprehensive mechanistic studies to complement efforts of experimental works towards this ultimate goal is lacking [29].

Though several efforts have been made in synthesizing various derivatives of isoxazolidines, to the best of our knowledge the only method reported in the literature for the construction of cyclobutane-condensed isoxazoline systems is the Bianchi's tandem sequential $[4 + 2]/[3 + 2]$ cycloaddition of COTE with dimethyl acetylenedicarboxylate and nitron derivatives [16]. However, there is no mechanistic study on this useful reaction to rationalize reactivity and the origin(s) of the regio- and stereo-selectivities of the reaction. Additionally, no report has been made on the effects of substituents on the mechanistic pathways of the tandem Diels – Alder/ $1, 3 -$ dipolar cycloaddition of COTE with functionalized-alkynes and nitrones. Also, no experimental nor theoretical study has reported the synthetic prospects of changing the addition sequence to a $[3 + 2]/[4 + 2]$ cycloaddition of the dimethyl acetylenedicarboxylate with nitrones and COTE to ascertain how it may account for product outcomes, efficiency and improved selectivities. These mechanistic questions/issues are very crucial towards the syntheses of cyclobutane-condensed tricyclic pyrazolines of high selectivity and efficiency.

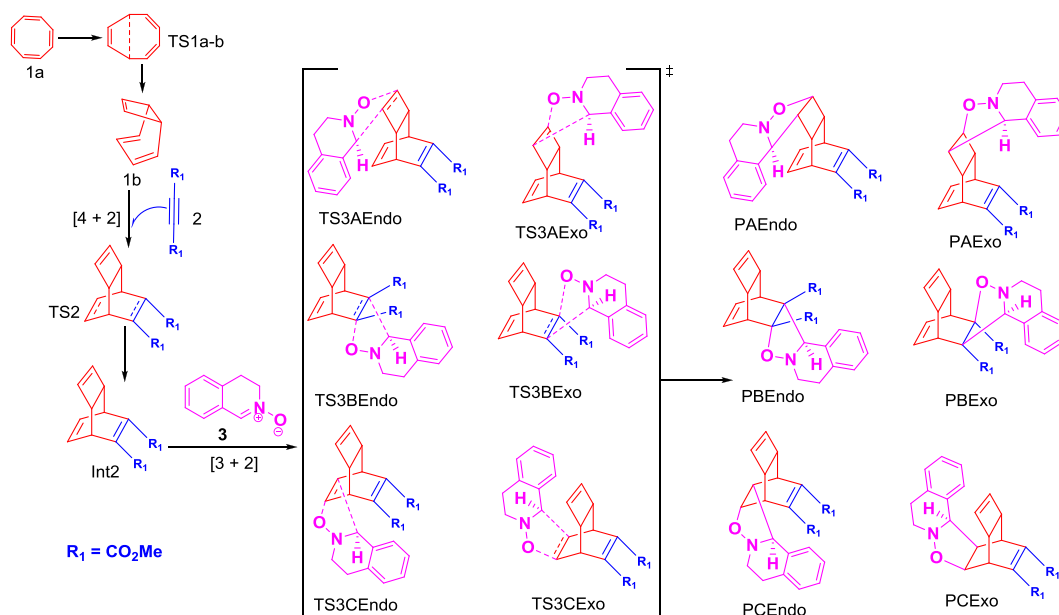
Herein, the potential energy surface is thoroughly explored by way of density functional theory (DFT) calculations to elucidate and shed light on the mechanisms of the tandem sequential $[4 + 2]/[3 + 2]$ and $[3 + 2]/[4 + 2]$ cycloaddition reaction of COTE with functionalized-alkynes and cyclic and acyclic nitrones towards the formation of isoxazolidine derivatives. Thermolysis of the tandem adducts is also explored. Our aim is to shed light on the molecular level mechanistic details of the reaction. The different reactivity of the cyclobutene and cyclohexadiene double bonds in the various adduct intermediates of this reaction are evaluated. Being mindful of the importance placed on the addition sequences in this class of reactions and how that affects product outcomes, several permutations hitherto unreported are extensively explored. Furthermore, this study investigates the effects of substituents on reactivity, regio-, and stereo-selectivities of these reactions. Schemes 3–9 as outlined below are employed in this comprehensive exploratory study.



Scheme 1. Tandem sequential cycloaddition of COTE with dimethyl acetylenedicarboxylate and 3,4-dihydroisoquinoline N-oxide as reported by Bianchi et al. [16].



Scheme 2. Tandem sequential $[4 + 2]/[3 + 2]$ cycloaddition of COTE with dimethyl acetylenedicarboxylate and acyclic nitrones as reported by Bianchi et al. [16].



Scheme 3. Proposed reaction pathways for the study of $[4 + 2]/[3 + 2]$ addition reaction of COTE with dimethyl acetylenedicarboxylate and a cyclic nitrone for the formation of tricyclic isoxazolidine derivatives.

2. Computational details and methodology

All the DFT computations were performed using the Spartan'14 [30] and Gaussian 09 [31] Molecular Modeling software packages at the M06-2X/6-311G(d,p) level of theory. The M06-2X functional developed by Zhao and Truhlar [32] is a hybrid meta-generalized gradient approximation (meta-GGA) established to be effective at computing thermochemical and kinetic parameters, especially where nonlocal dispersion interactions play a role [33–35]. In chemical transformations where dominant changes in C–C bond breaking and formation occurs, M06-2X generally avoids systematic errors associated with energetic barrier heights with, for instance, B3LYP [36]. Using the polarizable continuum model (PCM), benzene was employed to compute solvation effects in the reactions [37].

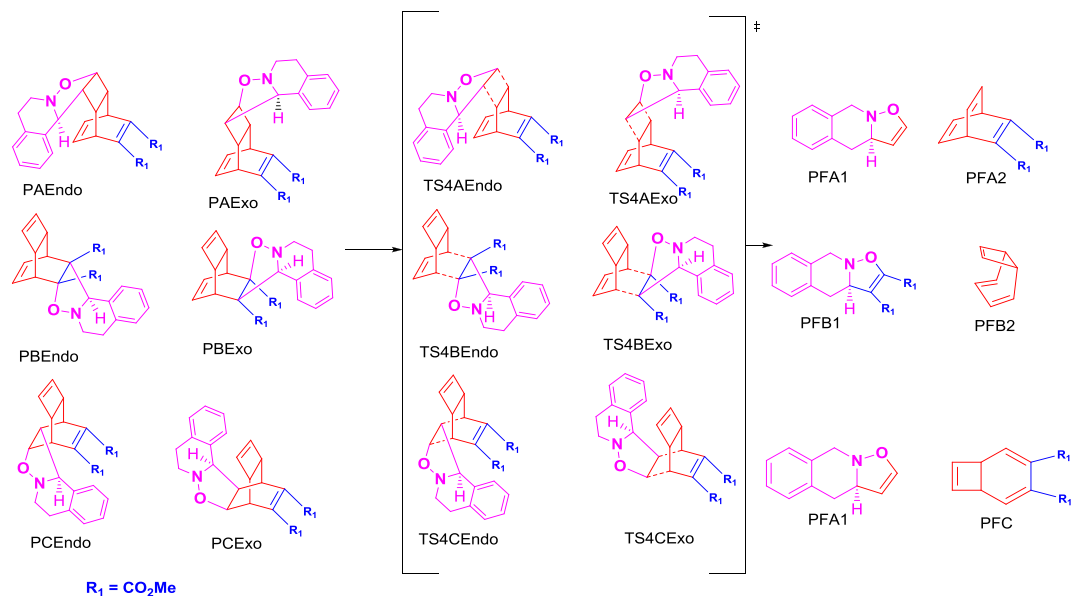
The initial geometries of the structures were built using Spartan's graphical model builder and minimized interactively using the sybyl force field [38]. Transition state structures were computed by first obtaining guess input structures. This was done by constraining specific internal coordinates of the molecules (bond

lengths, bond angles, dihedral angles) while fully optimizing the remaining internal coordinates. This procedure offers appropriate guess transition state input geometries which are then submitted for full transition state calculations without any geometry or symmetry constraints. Full harmonic vibrational frequency calculations were carried out to verify that each transition state structure had a Hessian matrix with only a single negative eigen value, characterized by an imaginary vibrational frequency along the respective reaction coordinates. Intrinsic reaction coordinate calculations were then performed to ensure that each transition state smoothly connects the reactants and products along the reaction coordinate [39–41].

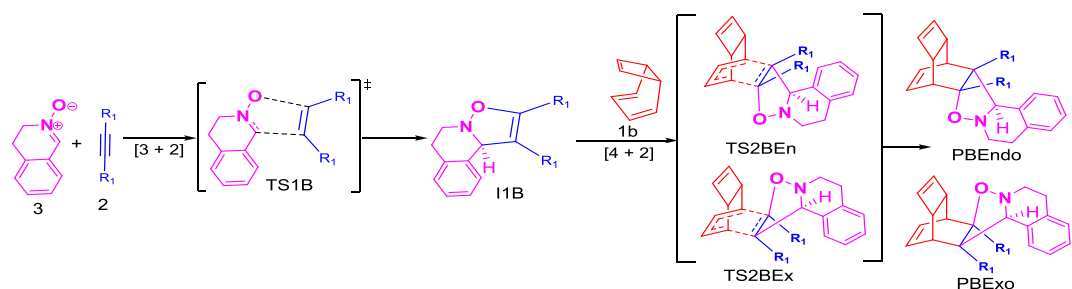
3. Results and discussion

3.1. $[4 + 2]/[3 + 2]$ tandem sequential cycloaddition reaction of COTE with 2 and 3

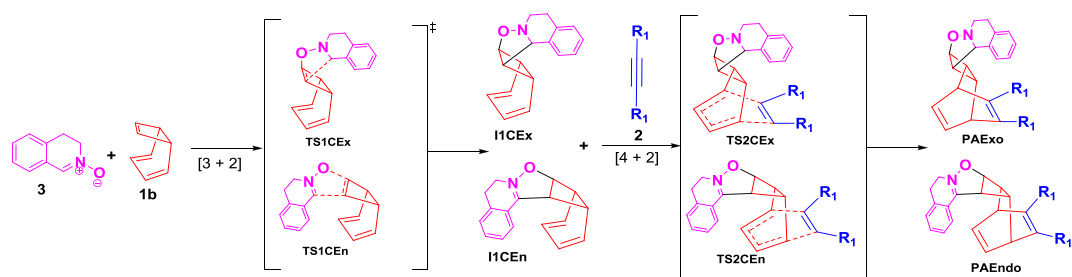
Scheme 3 outlines the proposed reaction pathways for the cycloaddition of dimethyl acetylenedicarboxylate with



Scheme 4. Proposed reaction pathways for the thermolysis of the [4 + 2]/[3 + 2] tandem adducts obtained from addition reaction of COTE with dimethyl acetylenedicarboxylate and a cyclic nitron.



Scheme 5. Proposed reaction pathways for the study of the tandem [3 + 2] addition reaction of a cyclic nitron and dimethyl acetylenedicarboxylate and follow up [4 + 2] addition of the adduct with COTE for the formation of tricyclic isoxazolidine derivatives.

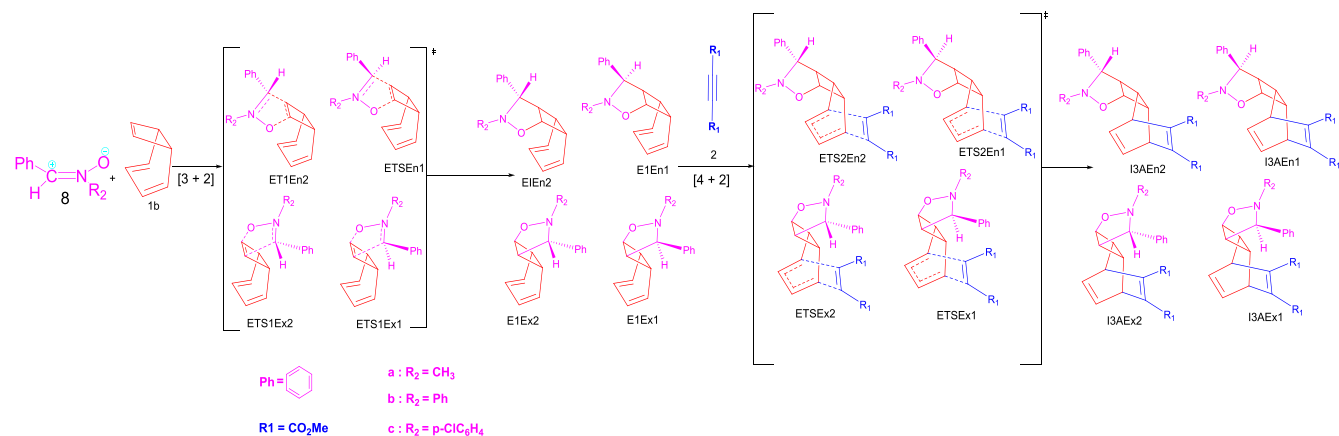


Scheme 6. Proposed reaction pathways for the study of the tandem [3 + 2] addition reaction of a cyclic nitron and COTE and follow up [4 + 2] addition of the adducts with dimethyl acetylenedicarboxylate for the formation of tricyclic isoxazolidine derivatives.

cyclooctatetraene (COTE), **1a** and 3,4-dihydroisoquinoline N-oxide (**3**). The reaction will most likely proceed by an initial electrocyclic ring closure of the COTE (**1a**) through **TS1** to generate a bicyclic intermediate, bicyclo [4, 2, 0] octa-2, 4, 7-triene (**1b**) [42] containing the 1,3-butadiene moiety. The *in situ* generated **1b** undergoes a Diels-Alder cycloaddition with **2** through transition state **TS2** to yield a dipolarophile intermediate **Int2**. This will be followed by a [3 + 2] cycloaddition (32CA) reaction between **Int2** and **3**. The addition of **3** and **Int2** in the [3 + 2] fashion is proposed to take place across either the cyclobutene or the cyclohexadiene double bonds of the Diels-Alder adduct in various regio- and stereo-

isomeric modes to yield their corresponding cyclobutane-condensed tricyclic isoxazolidines derivatives. It should be noted that whenever the incoming dipole attacks the dipolarophile (**Int2**) in the same configuration/plane with the bridging cyclobutene ring, it is considered *exo* whereas attacks from directly opposite the bridging ring is considered as an *endo* isomer.

Fig. 1 shows the zero-point-corrected Gibbs free energy profile as well as the optimized geometries of the stationary points (minima and maxima) relevant to the proposed scheme of study of the [4 + 2]/[3 + 2] addition of the **2** with COTE derivatives (**1a** and **1b**) and a cyclic nitron (**3**). All the calculations were carried out in



Scheme 9. Proposed reaction pathways for the study of the tandem [3 + 2] addition reaction of acyclic nitrones and COTE and follow up [4 + 2] addition of the adducts with dimethyl acetylenedicarboxylate for the formation of tricyclic isoxazolidine derivatives.

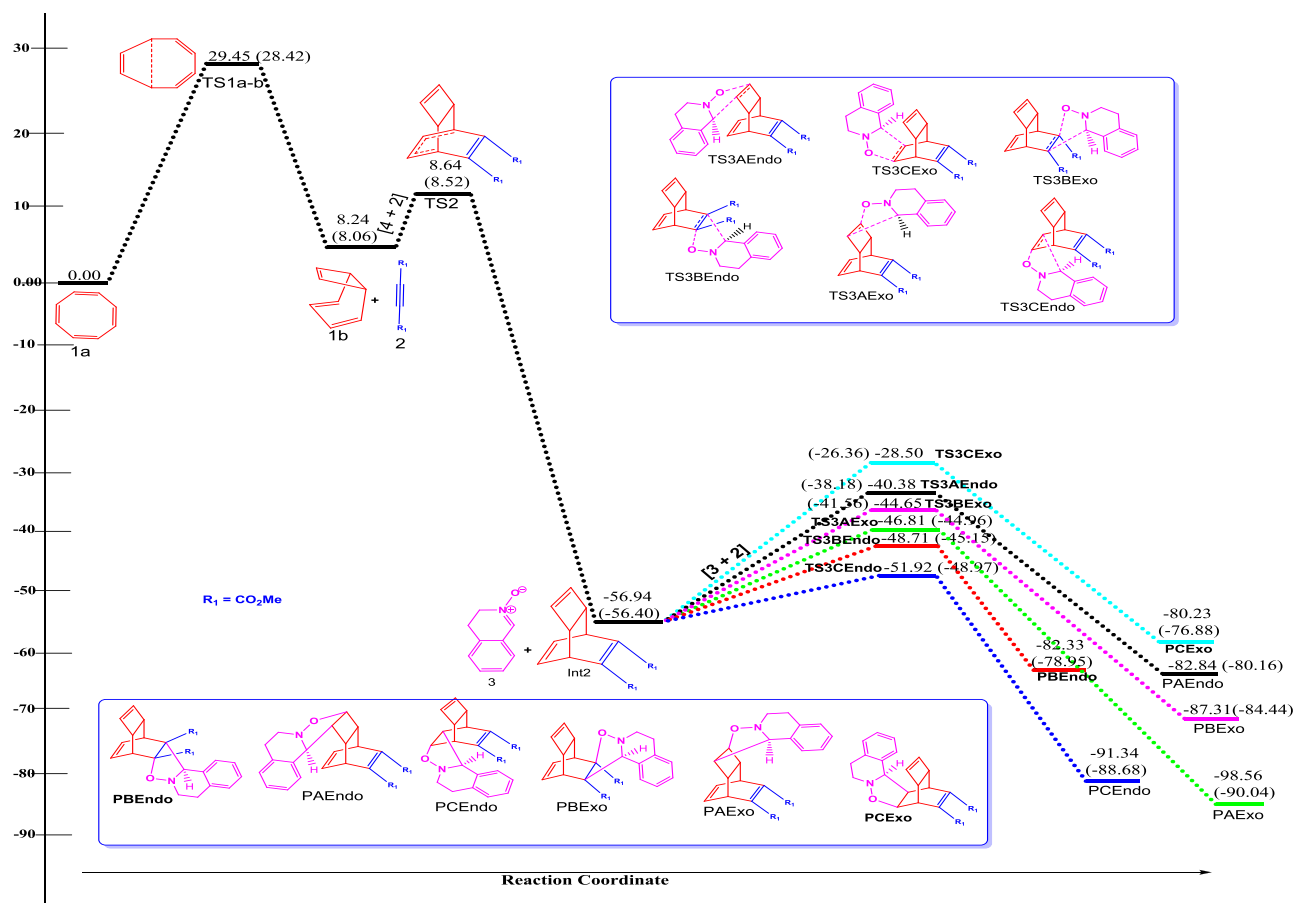


Fig. 1. Zero point energy corrected Gibbs free energy profile of the [4 + 2]/[3 + 2] addition of dimethyl acetylenedicarboxylate with COTE and 3,4-dihydroisoquinoline N-oxide in gas phase at the M06-2X/6-311G(d,p) level of theory. Results for computations in benzene at 298.15 K are in parenthesis. All relative energies in kcalmol⁻¹.

isolation. These observations give an indication that the reactivity of the cyclobutene and the cyclohexadiene double bands are very competitive. The results indicate that the addition of the dipole across the unsubstituted double bond in the cyclohexadiene moiety in **Int2** is the most stable pathway since it recorded the least activation barrier (**TS3CEn2** = 5.02 kcal/mol). The substituted double bond in the cyclohexadiene is the next most reactive since it recorded an activation energy of 8.23 kcal/mol (**TS3BEn2**). **PAExo**

formation, which arises from addition of the dipole to the cyclobutene double bond in the dipolarophile in the *exo* fashion was found to be the third most favoured route with an activation energy of 10.13 kcal/mol in the gas phase.

It should be noted that both **PCEn2** and **PBEn2** formation arises from an *endo* approach of the dipole. This observation could be attributed to the steric encumbrance of **Int2** which makes an *endo* attack a likely favourable approach. Again, for **PAExo**

formation the favourability of the *exo* attack could be mainly due to steric interactions. These observations are thoroughly investigated in a latter section of this study.

3.2. Thermolytic breakdown of the tandem adduct to other synthetic analogues

Fig. 2 shows the optimized geometries of the stationary points (minima and maxima) as well as the zero-point-corrected Gibbs free energy profile relevant to the proposed thermolysis of the tandem adducts obtained from the $[4 + 2]/[3 + 2]$ cycloaddition of **1b** and **2** with **3**. The computations were carried out both in gas phase and solvent (benzene). Results for the solvent phase calculations are reported in parenthesis (Fig. 2).

It is observed that the thermolytic cleavage of **PAExo** and **PAEndo** adduct occurs with very high activation barriers (84.61 kcal/mol and 74.58 kcal/mol respectively) leading to fragments **PFA1** and **PFA2** with reaction energy of -52.75 kcal/mol in the gas phase. Thermolytic breakdown of **PBEndo** and **PBExo** also occur via **TS4BEndo** and **TS4BExo** with activation barriers of 49.43 kcal/mol and 51.41 kcal/mol respectively leading to formation of **PFB1** and **PFB2** fragments with reaction energy of -66.90 kcal/mol. It is worth noted that **TS4BEndo** and **TS4BExo** proceed via a retro-Diels-Alder addition. Also, cleavage of the pyrrole linkage in **PCEndo** and **PCExo** has been found to occur via **TS4CEndo** and **TS4CExo** with activation barriers of 60.42 kcal/mol and 55.4 kcal/mol leading to **PFC** and **PFA1**. **PFC** and **PFA1** have a reaction energy of -74.27 kcal/mol, being the most stable among the thermolytic fragments. From the study, it can be said that the thermolytic cleavage of the tandem adducts proceed generally with very high activation barriers. It is worth noting that, the ring opening of **PFC**

will lead to the formation of dimethyl phthalate (**13**) as shown in Scheme 2.

In spite of the high-energy requirements, Bianchi et al. [16] have used this route to access tricyclic and less strained isoxazolidines (**PFA1** and **PFB1**) as well as other synthetic analogues (**PFA2**, **PFB2** and **PFC**). In the subsequent section, we will explore the possibility of obtaining some of these useful thermolytic fragments in a rather direct approach using the same reaction substrates.

3.3. Investigating the effect of change in addition sequence on kinetics and product outcomes

As part of an ongoing study in our group [40,41], we have established that generally, in tandem sequential addition reactions the order of the addition greatly affects selectivity and hence product outcomes.

Herein, we explore the possibility of a $[3 + 2]/[4 + 2]$ addition sequences using the same reaction substrates. Fig. 3 shows the zero-point-corrected Gibbs free energy profile as well as the optimized transition states and equilibrium geometries located on the potential energy surface (PES) of a 32CA between **3** and **2** to form **I1B**. This is followed by a Diels-Alder (DA) addition of **I1B** to **1b** to form the corresponding tandem adducts. From Fig. 3 it is seen that addition of **3** to **2** proceed with an energy barrier of 9.80 kcal/mol to form **I1B** with a reaction energy of -39.60 kcal/mol. A prime advantage of this addition sequence is that regioselectivity is no longer an issue. This observation completely limits the possible isomers to only two (**TS2BEn** and **TS2BEx**) compared to six isomers in the original $[4 + 2]/[3 + 2]$ addition sequence reported by Bianchi and his co-workers [16]. The DA addition of **I1B** with **1b** occurs via **TS2BEn** and **TS2BEx** with activation barriers of 7.22 kcal/

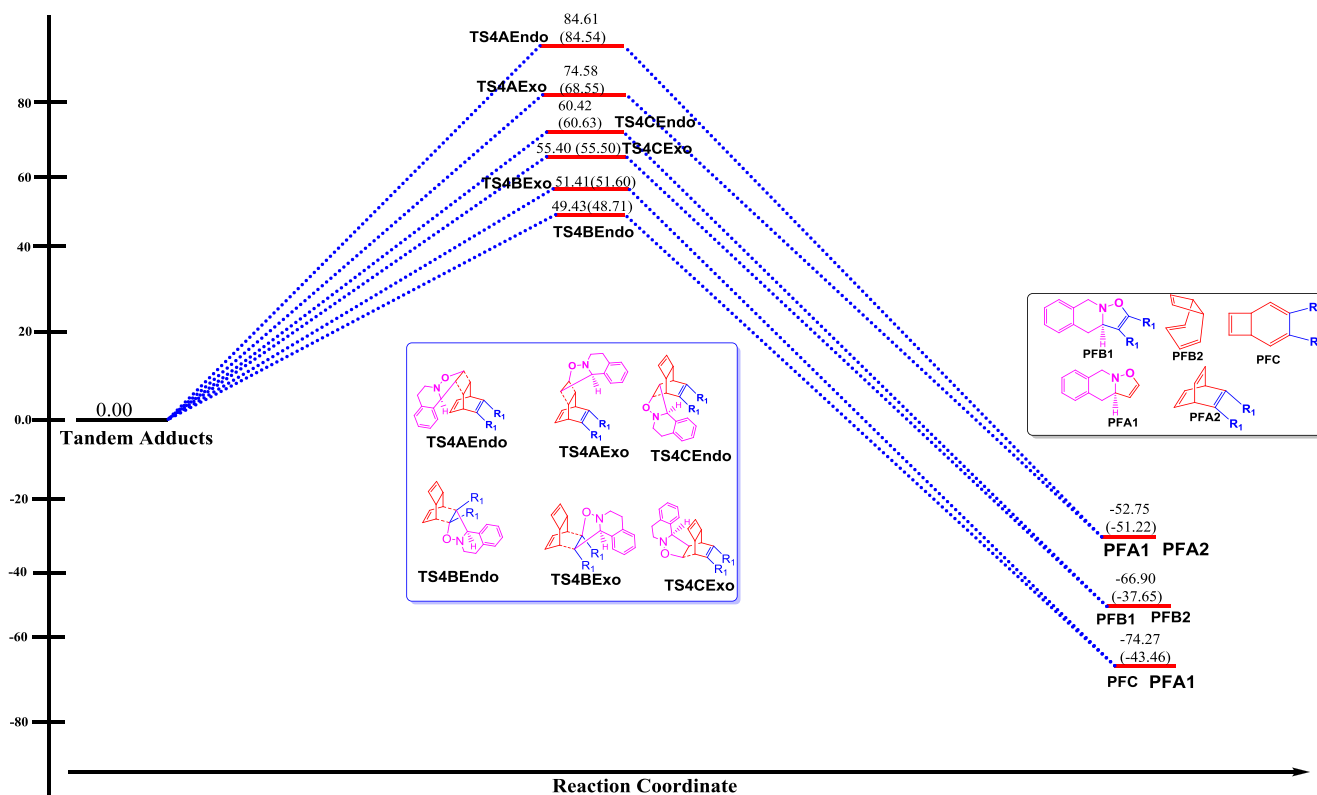


Fig. 2. Zero point energy corrected Gibbs free energy profile for the thermolytic breakdown of the $[4 + 2]/[3 + 2]$ tandem adducts obtained from the addition of dimethyl acetylenedicarboxylate (**2**) with COTE derivative (**1b**) and 3,4-dihydroisoquinoline N-oxide (**3**) in gas phase at the M06-2X/6-311G(d,p) level of theory. Relative energies in kcalmol⁻¹. Results for computations in benzene at 298.15 K are in parenthesis. All energies are relative to their respective tandem adduct.

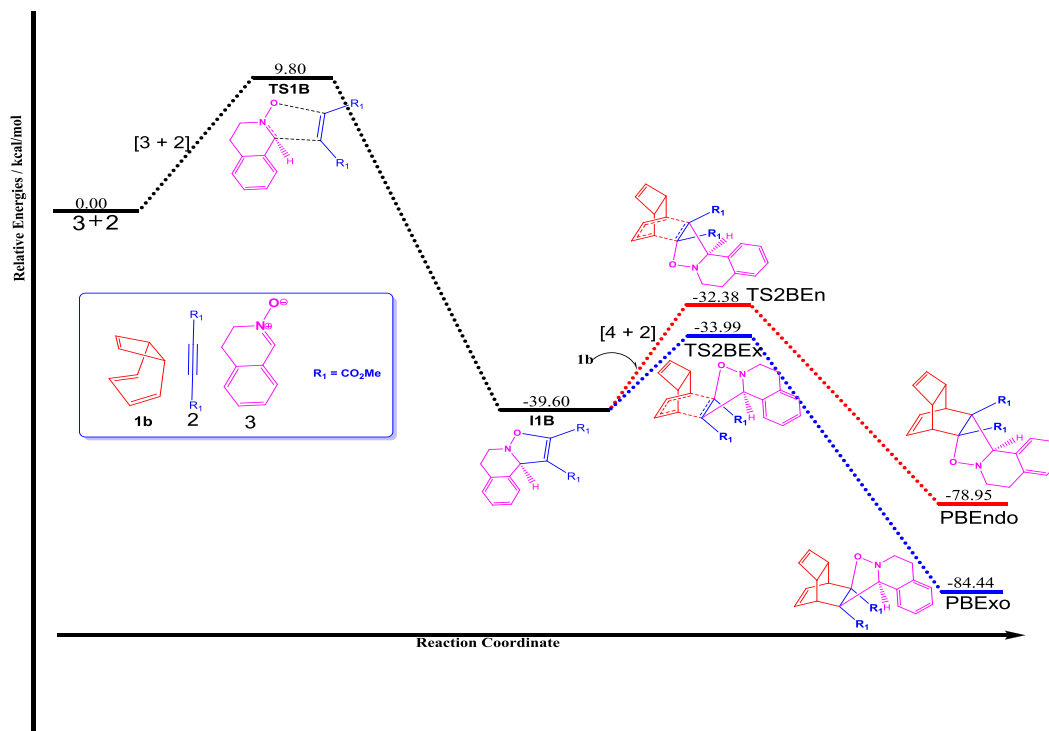


Fig. 3. Zero point energy corrected Gibbs free energy profile of the [3 + 2]/[4 + 2] addition reaction of 3,4-dihydroisoxanoline N-oxide (**3**) with dimethyl acetylenedicarboxylate (**2**) and COTE derivative (**1b**) at the M06-2X/6-311G(d,p) level of theory. Relative energies in kcalmol⁻¹. All computations were carried out in benzene at 298.15 K.

mol and 5.61 kcal/mol respectively. These pathways lead to **PBEndo** and **PBExo** with reaction energies of -39.35 kcal/mol and -44.84 kcal/mol respectively. From the energy profile (Fig. 3), formation of **PBExo** is the most favoured both in terms of kinetics and product stabilities.

Here it should be noted that just by changing the sequence of the addition, the product formation is limited to only **PBEndo** and **PBExo** with **PBExo** being the most favoured. Hence, for the formation of **PBExo** and **PBEndo** isomers, we proposed that this approach is the best to employ. Again, it is seen that the 32CA adduct **I1B** is obtained with a good stability. Hence, this comes as a convenient route for obtaining less strained tricyclic isoxazolidines (**I1B**) compared to the rigorous approach adopted by Bianchi et al. [16,17]. In their approach **I1B** which is the same as the thermolytic fragment **PFA1** (see Scheme 4 and Fig. 2) could only be obtained by thermolysis of the tandem adducts.

Fascinated by the observations so far, we extended the study to explore the possibility of an initial 32CA of and **1b** and **3** to form **I1En** and **I1Ex**. This will be followed by a DA addition of the dipolarophile obtained with **2** for stereoselective formation of **PAEndo** and **PAExo**. Fig. 4 displays all the relevant optimized structures as well as Gibbs free energy profile involved in the 32CA reaction of **3** and **1b** and a follow up [4 + 2] addition reaction. Cycloaddition of **3** and **1b** takes place via **TSICEn** and **TSICEx** with activation barriers of 12.45 kcal/mol and 11.52 kcal/mol respectively suggesting a favourable pathway for *exo* attack (**TSICEx**). The 32CA adduct also gave **I1CEx** as the most stable (-33.49 kcal/mol) alongside **I1CEn** with reaction energy of -30.37 kcal/mol. The subsequent [4 + 2] addition of **2** to the initial 32CA adduct is found to proceed via **TS2CEn** and **TS2CEx**. **TS2CEx** has an activation energy of 7.82 kcal/mol leading to **PAExo** with reaction energy of -56.55 kcal/mol while **TS2CEn** also has an energy barrier of 11.80 kcal/mol leading to **PAEndo** with a reaction energy of -49.79 kcal/mol. Here it should be noted that by employing our proposed addition

sequence, **PAEndo** and **PAExo** are the only possible products. Hence, this addition sequence suggests improved selectivity in the reaction pathways.

3.4. Investigating the regioselectivity of the reactions

In the [4 + 2]/[3 + 2] cycloaddition between **1a**, **2** and **3**, regioselectivity occurs at the 32CA addition step (see Scheme 3) since the dipole could add across the olefin bond in the cyclobutene subunit or across either of the substituted or the unsubstituted double bond in the cyclohexadiene subunit. In this section of our study, perturbation molecular orbital (PMO) theory is employed [43] to rationalize both the reactivity and the regioselectivity in the 32CA of **Int2** and **3**.

Fig. 5 is a depiction of all the possible orbital interactions in **Int2** and **3** to aid in a better conception of the PMO approach. We envisaged a possible HOMO_{dipole} – LUMO_{dipolarophile} interaction as well as that of HOMO_{dipolarophile} – LUMO_{dipole}. The orbital energy obtained for the HOMO_{dipole} – LUMO_{dipolarophile} interaction is 6.332 eV and that of HOMO_{dipolarophile} – LUMO_{dipole} is 7.577 eV. Hence, the dominating orbital interactions will take place between the HOMO of the dipole and the LUMO of the dipolarophile since our calculations show that it is the interaction with closest energy, implying a normal electronic demand cycloaddition reaction.

From this point, we subjected the dipole and the dipolarophile to a normal bond order analysis. Analyses of the molecular orbital coefficients in the cycloaddition centres show that, for the dipole (**3**) $O_{19} = -0.554$ and $C_{11} = +0.002$ whereas in the dipolarophile (**Int2**), $C_1 = -0.180$, $C_3 = -0.186$, $C_9 = -0.069$, $C_{10} = -0.049$ while $C_{15} = -0.177$ and $C_{17} = -0.178$. The various atomic labels in **Int2** and **3** are shown in Fig. 6. Houk's rule [44] states that for a normal electronic demand cycloaddition reaction the addition will occur between atoms with the highest molecular orbital coefficients since that will lead to interaction with the greatest stabilization.

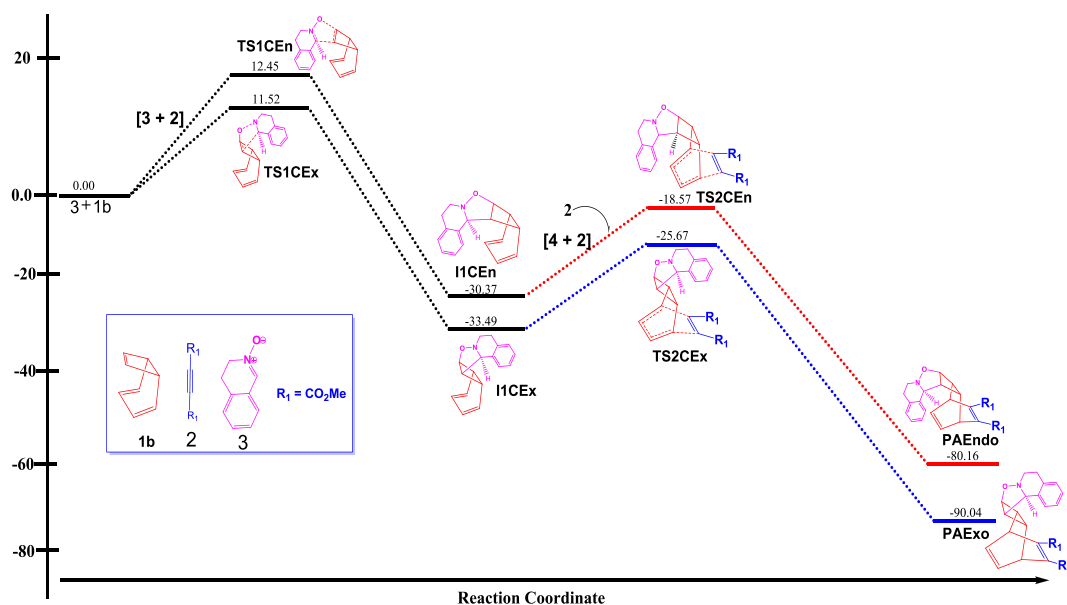


Fig. 4. Zero point energy corrected Gibbs free energy profile of the [3 + 2]/[4 + 2] addition reaction of 3,4-dihydroisoquinoline N-oxide (**3**) with COTE derivative (**1b**) and dimethyl acetylenedicarboxylate (**2**) at the M06-2X/6-311G(d,p) level of theory. Relative energies in kcalmol⁻¹. All computations were carried out in benzene at 298.15 K.

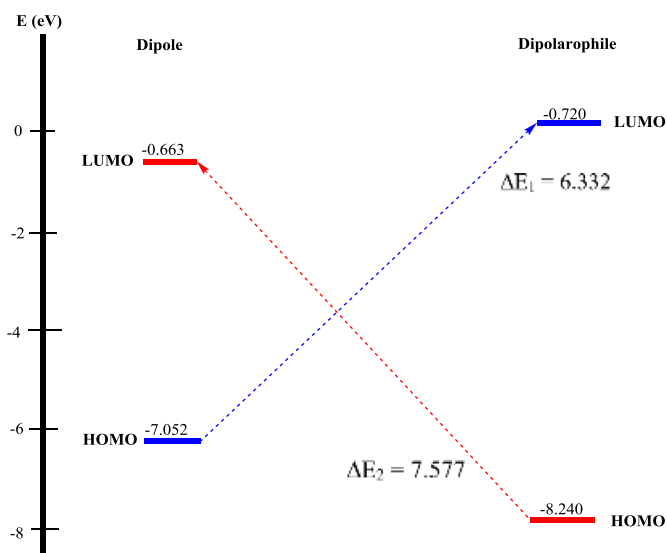


Fig. 5. Frontier molecular orbital interactions in the 32CA reaction of **Int2** and **3** at the M06-2X/6-311G(d,p) in benzene.

Therefore, arguing from our normal bond order analysis, the addition of the dipole across the olefinic C₁-C₃ bond of the dipolarophile will be the most favourable point of attack followed by C₁₅-C₁₇ and C₉-C₁₀ which agrees well with the experimentally observed products distributions [16]. The PMO results is also in good agreement with the trends obtained from the activation barriers.

3.5. Investigation of the origin of endo/exo selectivities in the [4 + 2]/[3 + 2] addition of **1b**, **2** and **3**

From Scheme 3, it can be seen that at the [3 + 2] cycloaddition step, each regioisomer has two possible transition states leading to six different tandem adducts. Based on the activation energies, it has been established that TS3CEndo is the most preferred route

since it recorded the least activation energy (Fig. 1).

Again, the perturbation molecular orbital (PMO) theory is invoked [43] to rationalize this observation. Fig. 7 shows the graphical illustration of the HOMOs of all the six possible transition state. It can be seen that there is a migration of the electron density from the dipole to the dipolarophile in all instances.

An evaluation of the HOMO – LUMO gaps of all the six possible endo/exo selective transition states computed with at the M06-2X/6-311G(d,p) in benzene reveal that TS3AEndo has an energy gap of 6.52 eV, TS3AExo = 6.47 eV, TS3BEndo = 6.80 eV, TS3BExo = 6.90 eV, TS3CEndo = 6.04 eV and TS3CExo = 6.11 eV. Thus, the HOMO – LUMO gap of TS3CEndo has the least energy requirement among all the six transition states, hence the most favourable interaction.

3.6. The reactivity and selectivity in the reaction of acyclic nitrones with **1b** and **2**

In order to enhance the scope of our study, we investigated the reactivity of acyclic nitronone derivatives (**8a**, **8b**, **8c**) with **1b** and **2** in various addition sequences.

A thorough DFT exploration of the PES for the tandem sequential [4 + 2]/[3 + 2] addition reaction of **1b** with **2** and **8** characterized twelve plausible transition states leading to their corresponding tandem adducts (Scheme 7). The follow-up thermolytic cleavage of the tandem adducts is also found to proceed via twelve plausible transition states towards formation of various monocyclic isoxazolidines and other synthetic analogues. Results for the reaction of the derivatives of the acyclic nitrones considered in this study with **1b** and **2** formation of the tandem adducts are reported in Tables 1 and 2. Also, the energetics for the subsequent thermolysis of the tandem adducts are also reported in Tables 3 and 4.

Based on the activation barriers (see Table S1), it is realized that the initial cyclization of **1a** proceed through activation height of 8.24 kcal/mol to yield **1b** with thermodynamic stability of 29.45 kcal/mol (see Table S2). This is followed by a rapidly occurring [4 + 2] addition sequence of **1b** with **2** through activation barriers of merely 0.39 kcal/mol to form **12**. Reaction of **8a** (N-methyl-C-phenylnitronone) with **12** could occur through twelve possible

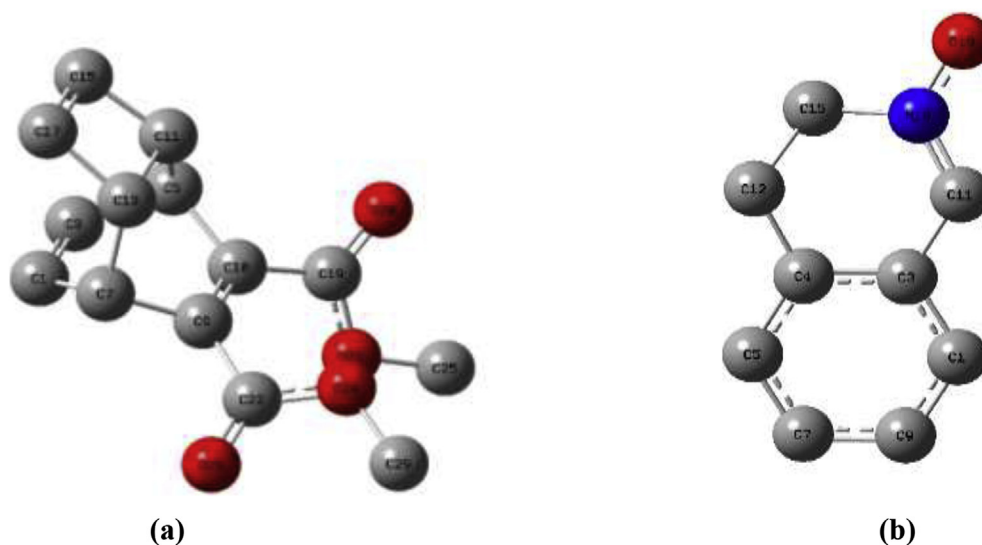


Fig. 6. Graphical display of atomic labels on **Int2** (a) and **3** (b) respectively. Hydrogen atoms are ignored for clarity.

transition states. **T3BEn2a** is the most favoured pathway with an activation barrier of 9.97 kcal/mol leading to the formation of **I3Bn2a** with a reaction energy of -20.56 kcal/mol (Table S2). Our results show that all the tandem cycloadducts have higher thermodynamic stability values indicating a non-reversible addition sequence. Hence, the product expected to be observed from this reaction will most likely depend solely on the activation barriers.

Although it has been speculated elsewhere [17] that the substituted double bond in the cyclohexadiene subunit in the dipolarophile (**12**) shows no reactivity towards nitrones, this observation is strongly disputed by our calculations. A brief inspection of Table S1 shows that, among all the transition states leading to the tandem adducts, **T3BEn2** is the most favoured in the case of **8a** reactivity. The same trend is observed when the study was repeated in benzene (Tables 1 and 2). However, changing the acyclic nitron to N-phenyl-C-phenylnitron (**8b**), it was observed that **T3Cn2b** is the most favoured (7.52 kcal/mol) followed by **T3BEn1b** and **T3AEx1b**. In addition, **8c** reactivity revealed that **T3CEn2c** is the most favoured followed by **T3Ax1c** and **T3BEn1c**. Based on the forgoing energetic trends, it can be established that the reactivity of the acyclic nitrones considered in this work is greatly affected by the type of substituent on the nitrogen as earlier mention elsewhere [16].

We extended the study to cover the thermolysis of the tandem adducts through the fourth isomeric transition states (Scheme 7) to form their respective thermolytic fragments. The results of this section of our study are summarized in Tables 3 and 4. From Table S3, it can be seen that generally the thermolytic cleavage proceed with very high activation energies irrespective of the nitron used (**8a**, **8b**, **8c**). Although, solvent effects are computed, it is seen that it has insignificant effects on the energetic trends. Also, from Table S4 it can be seen that the reaction energies obtained for all the thermolytic fragments are lower relative to the tandem adducts. This observation suggests that the thermolytic breakdown is controlled by both kinetic and thermodynamic factors.

Actuated by the high energetic barriers as well as product instabilities of the thermolysis step, we made a thorough exploration of how changing the addition sequence will open the gateway for easier access to thermolytic fragments as well as the tandem adducts. Hence, the subsequent sections are devoted towards this objective.

3.7. [3 + 2] cycloaddition of **8a** with **2** and follow-up [4 + 2] addition of the adduct to **1b**

Fig. 8 illustrates the optimized geometries as well as the relative energies of all the stationary points involved in the [3 + 2] cycloaddition of **8a** with **2** and follow-up [4 + 2] addition of the adduct to **1b**. It is seen that the transformation of **8a** and **2** to **P11a** and **P12a** requires activation energies of 6.6 kcal/mol and 5.71 kcal/mol respectively. It should also be noted that **P11a** and **P12a** corresponds to the thermolytic fragments **PB2a** and **PB1a** (Scheme 7). Hence, our explored mechanistic addition sequence has offered a less energy-demanding approach towards obtaining monocyclic isoxazolidines which was otherwise obtained via thermolysis of the tandem adducts involved in Bianchi et al. [16,17] addition sequence found to proceed with very high activation barriers (mostly above 50 kcal/mol). It should be noted that the monocyclic isoxazolidines **P11a** and **P12a** are stable enough to merit isolation (-47.96 kcal/mol and -49.08 kcal/mol) respectively. Follow-up [4 + 2] addition of **P11a** and **P12a** to **1b** revealed a characterization of four possible mechanistic channels to yield four plausible tandem adducts. The tandem adducts (**I3BEn1a**, **I3BEn2a**, **I3BEx1a**, **I3BEx2a**) are stable enough, ruling out the possibility of a reversible process. Hence, product formation is solely dependent on the activation energies. **PTS2Ex2a** is found to be the most favoured channel with an energy barrier of 12.97 kcal/mol. Here also, it is seen that by changing the cycloaddition sequences the plausible product outcomes (tandem adducts) is reduced to only four isomers, indicating an improved reaction pathways.

3.8. [3 + 2] cycloaddition of **8a** with **1b** and follow-up [4 + 2] addition of the adduct to **2**

Intrigued by the outcome so far, we explored the mechanistic possibility of a 32CA reaction of **1b** with **8a** and follow-up DA addition to **2**. Fig. 9 is a display of all the optimized geometries of the stationary points (minima and maxima) as well as the zero-point-corrected Gibbs free energy profile relevant to the proposed 32CA reaction of **1b** with **8a** and follow-up DA addition to **2**. It can be seen that the reactivity of **8a** with **1b** can occur via **ETSen1**, **ETEn2**, **ETEx1** or **ETEx2** to yield their corresponding intermediates. **ETEx1** is the most favourable route with an activation barrier of 13.77 kcal/mol. The [3 + 2] adducts obtained are very

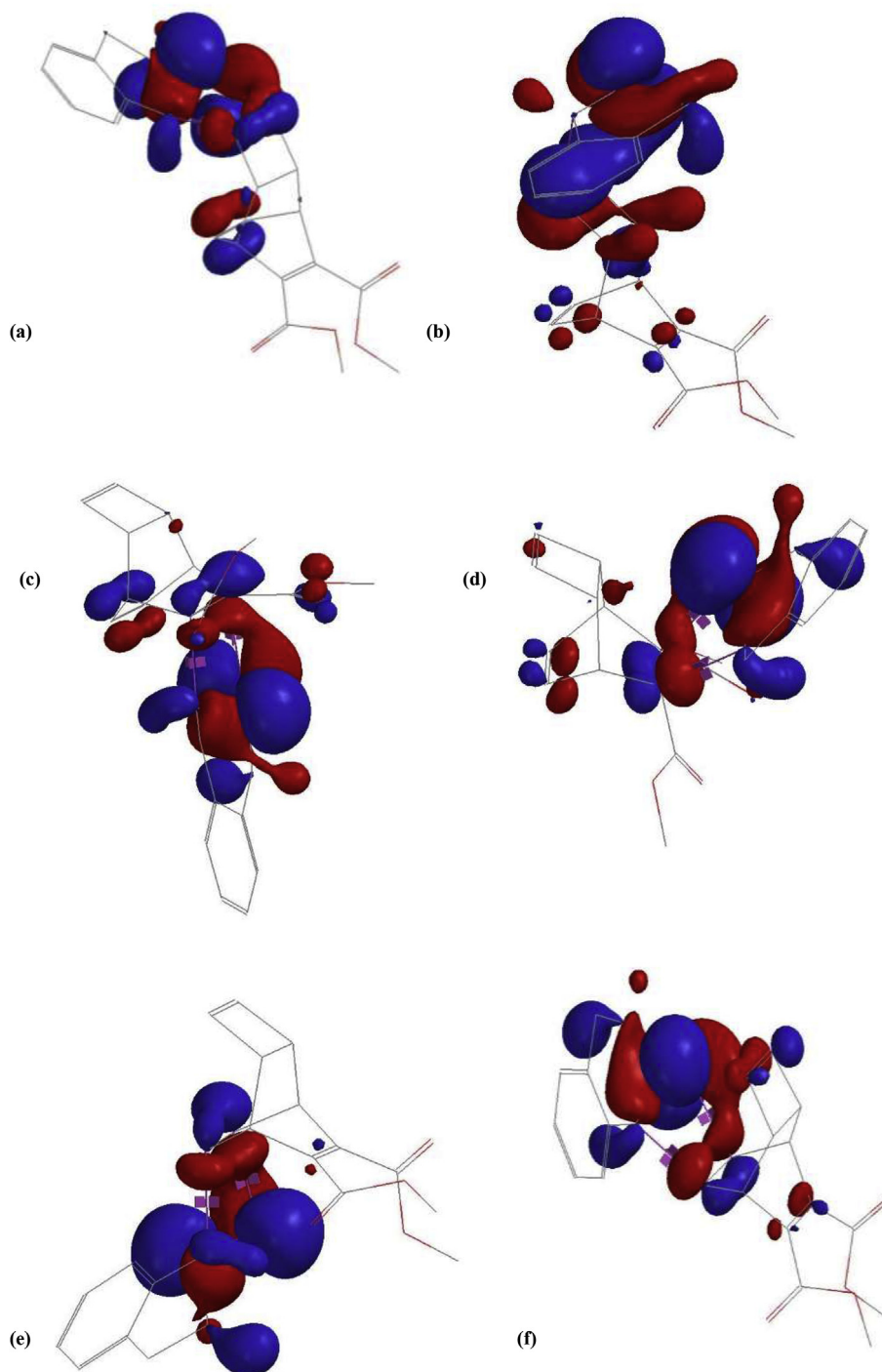


Fig. 7. Graphical depiction of the HOMOs of **TS3AEndo** (a), **TS3AExo** (b) **TS3BEndo** (c) and **TS3BExo** (d) **TS3CEndo** (e) **TS3CExo** (f) at the M06-2X with the 6-31G(d) basis set. Hydrogen atoms are ignored for clarity purposes.

stable and could be isolable with thermodynamic stabilities ranging from -30.07 kcal/mol to -33.25 kcal/mol. The 32CA adducts offer new class of isoxazolidine derivatives (**EIEn1**, **EIEn2**, **EIEx1**, **EIEx2**) thitherto not obtained from the experimental studies. Subsequent Diels-Alder addition of the 32CA adducts with **2** is predicted to proceed through four possible transition states (**ETS2En1**, **ETS2En2**, **ETS2Ex1**, **ETS2Ex2**). Among all the four, **ETS2x2** is the most preferred pathway with an activation energy of 8.43 kcal/mol. This step eventually yields four possible tandem

adducts (**I3AEn1**, **I3AEn2**, **I3AEx1**, **I3AEx2**). Formation of **I3AEx2** is found to be the most the most favoured with a reaction energy of -68.69 kcal/mol. Here also, our explorative mechanistic addition sequence has revealed another convenient and direct approach towards formation of cyclobutene-condensed tricyclic isoxazolidine systems with improved selectivity. The zero-point corrected Gibbs free energies and the cartesian coordinates of all the computed structures are shown in [Tables S5–S13](#) in the supporting electronic information.

Table 1
Activation barriers involved in the tandem [4 + 2]/[3 + 2] cycloaddition reaction of dimethyl acetylenedicarboxylate with cyclooctatetraene and acyclic nitrones (8a, 8b and 8c) at the M06-2X with the 6-311G(d,p) basis set. All energies are measured in kcalmol⁻¹.

[4 + 2]/[3 + 2] Tandem Addition														
Substituent		Activation Energies(ΔG^\ddagger)/kcal/mol												
R ₁	T1	T2	T3AEn1	T3AEn2	T3AEx1	T3AEx2	T3BEn1	T3BEn2	T3BEx1	T3BEx2	T3CEn1	T3CEn2	T3CEX1	T3CEX2
CH ₃	+29.45	+0.39	+21.27	+24.83	+11.61	+13.21	+11.99	+9.97	+16.81	+18.55	+12.23	+10.96	+30.40	+23.16
^a CH ₃	+28.42	+0.55	+19.24	+22.78	+9.47	+10.85	+10.53	+8.07	+14.60	+16.86	+10.43	+9.27	+28.41	+21.23
Ph	+29.45	+0.39	+19.72	+20.92	+8.73	+11.40	+8.29	+11.86	+16.84	+13.85	+11.10	+7.52	+28.84	+21.60
p-ClC ₆ H ₄	+29.45	+0.39	–	+20.59	+8.31	+11.05	+8.36	+11.24	+16.58	+13.71	+10.50	+2.34	+28.17	+21.07

^a Energetics in benzene at 298.15 K.

Table 2
Reaction Energies involved in the tandem [4 + 2]/[3 + 2] cycloaddition reaction of dimethyl acetylenedicarboxylate with cyclooctatetraene and acyclic nitrones (8a, 8b and 8c) at the M06-2X with the 6-311G(d,p) basis set. All energies are measured in kcalmol⁻¹.

[4 + 2]/[3 + 2] Tandem Addition														
Substituent		Reaction Energies(ΔG_{rxn})/kcal/mol												
R ₁	1b	12	13AEn1	13AEn2	13AEx1	13AEx2	13BEn1	13BEn2	13BEx1	13BEx2	13CEn1	13CEn2	13CEX1	13CEX2
CH ₃	+8.24	-73.43	-18.1	-20.07	-24.29	-27.83	-16.62	-20.56	-23.2	-21.27	-25.9	-28.13	-15.83	-22.49
^a CH ₃	+8.08	-72.56	-20.12	-21.81	-26.22	-29.38	-17.47	-21.82	-24.38	-22.13	-27.99	-30.21	-17.41	-23.87
Ph	+8.24	-73.43	-19.19	-24.01	-32.21	-32.32	-23.88	-22.27	-23.64	-25.69	-26.42	-30.29	-22.08	-25.45
p-ClC ₆ H ₄	+8.24	-73.43	-20.24	-25.37	-32.89	-33.04	-24.51	-22.93	-24.7	-26.49	-27.6	–	–	-26.46

^a Energetics in benzene at 298.15 K.

Table 3
Activation Energies involved in the thermolysis of the [4 + 2]/[3 + 2] tandem adducts at the M06-2X with the 6-311G(d,p) basis set. All energies are measured in kcalmol⁻¹. All energies are relative to their respective reactants.

Thermolysis of the [4 + 2]/[3 + 2] Tandem Adducts													
Substrate		Activation Energies(ΔG^\ddagger)/kcal/mol											
R ₁	T4AEn1	T4AEn2	T4AEx1	T4AEx2	T4BEn1	T4BEn2	T4BEx1	T4BEx2	T4CEn1	T4CEn2	T4CEX1	T4CEX2	
CH ₃	–	+66.02	+71.67	+71.75	+45.50	+49.73	+49.92	+47.20	+61.05	+60.26	+56.34	+61.09	
^a CH ₃	+67.67	+65.57	+71.81	+71.52	+44.96	+49.66	+50.06	+46.81	+60.22	+59.72	+56.50	+60.80	
Ph	+67.85	+66.47	–	–	+49.67	+49.77	+49.03	+49.61	+62.02	+59.18	+55.90	+57.55	
p-ClC ₆ H ₄	+68.18	+66.54	+70.60	+70.91	+49.93	+49.37	–	+50.16	+62.45	–	–	+57.87	

^a Energetics in benzene at 298.15 K.

Table 4
Reaction Energies involved in the thermolysis of the [4 + 2]/[3 + 2] tandem adducts at the M06-2X with the 6-311G(d,p) basis set. All energies are measured in kcalmol⁻¹. All energies are relative to their respective reactants.

Thermolysis of the [4 + 2]/[3 + 2] Tandem Adducts						
Substituent		Reaction Energies(ΔG^\ddagger)/kcal/mol				
R ₁	P(A1+A3)	P(A2+A3)	P(B1+B3)	P(B2+B3)	P(A1+C)	P(A2+C)
CH ₃	-60.94	-59.32	-60.85	-59.33	-62.78	-61.15
^a CH ₃	-62.86	-61.26	-61.06	-59.54	-60.61	-59.00
Ph	-64.30	-64.30	-62.68	-62.68	-66.14	-66.14
p-ClC ₆ H ₄	-64.88	-64.88	62.81	-62.92	-66.72	-66.72

^a Energetics in benzene at 298.15 K.

4. Conclusions

This study reports an extensive theoretical investigation on the tandem sequential [4 + 2]/[3 + 2] and [3 + 2]/[4 + 2] cycloaddition sequences involving an alkyne with COTE and cyclic and acyclic nitrones for the formation of diverse isoxazolidine derivatives and other synthetic precursors. A thorough exploration of the PES has characterized several regio- stereo- and enantio-selective mechanistic channels involved in these reactions. A perturbation molecular orbital (PMO) analysis has established a normal electronic demand character for the reaction. It is also established that solvation effects do not play significant role in the determination of

product outcomes. Both gas phase and solvent phase full optimizations calculations gave analogous energetic trends. Exploration of the thermolytic breakdown of the tandem adducts to subsequent monocyclic, bicyclic and tricyclic adducts has revealed that it occurs generally with very high activation barriers making it an inconvenient synthetic approach. It has also been found that the initial electrocyclic ring closure of the COTE is the rate-determining step in the tandem sequential [4 + 2]/[3 + 2] addition sequence. Along the tandem sequential [4 + 2]/[3 + 2] addition sequence involving the cyclic nitron, the reactivity of the three olefinic bonds in the dipolarophile (**Int2**) is found to be in the order: unsubstituted cyclohexadiene double bond > substituted cyclohexadiene double

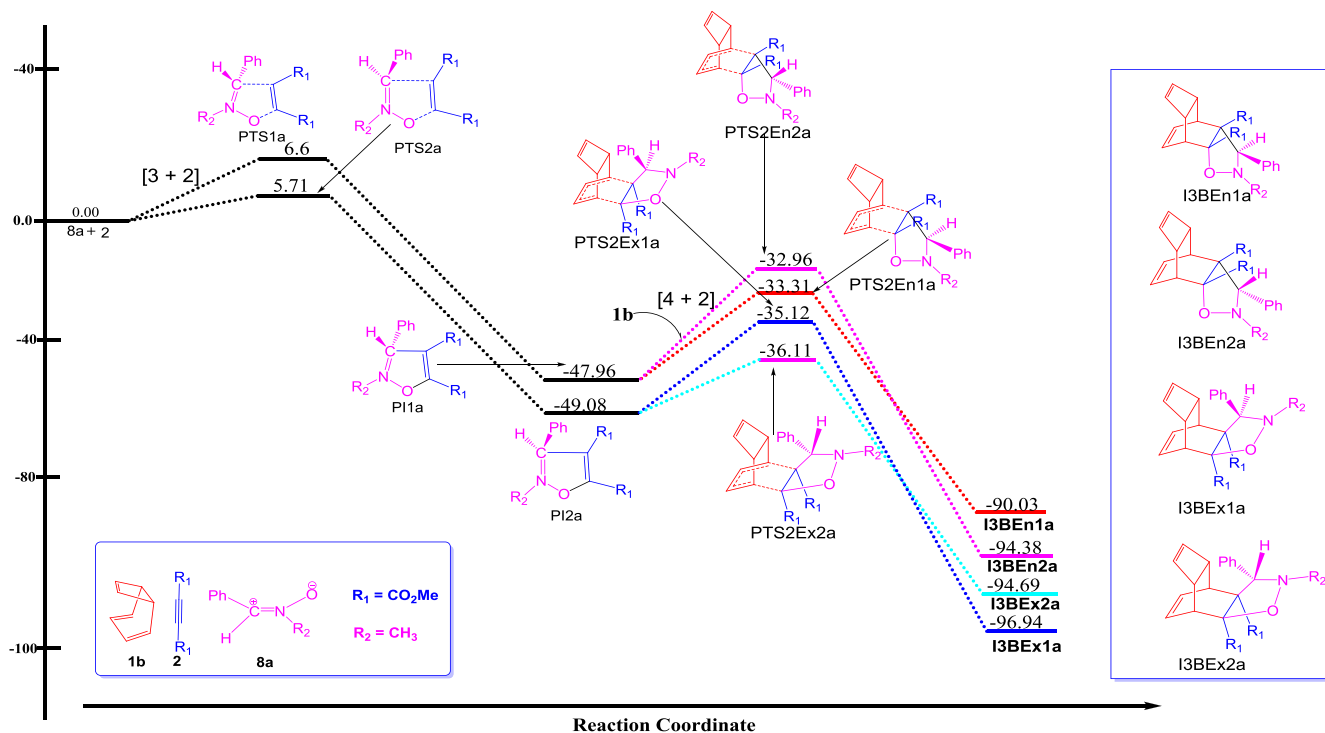


Fig. 8. Zero point energy corrected Gibbs free energy profile of the tandem [3 + 2] addition reaction of N-methyl-C-phenylnitron (**8a**) and dimethyl acetylenedicarboxylate (**2**) and follow up [4 + 2] addition of the adducts to COTE (**1b**) in benzene at the M06-2X/6-311G(d,p) level of theory.

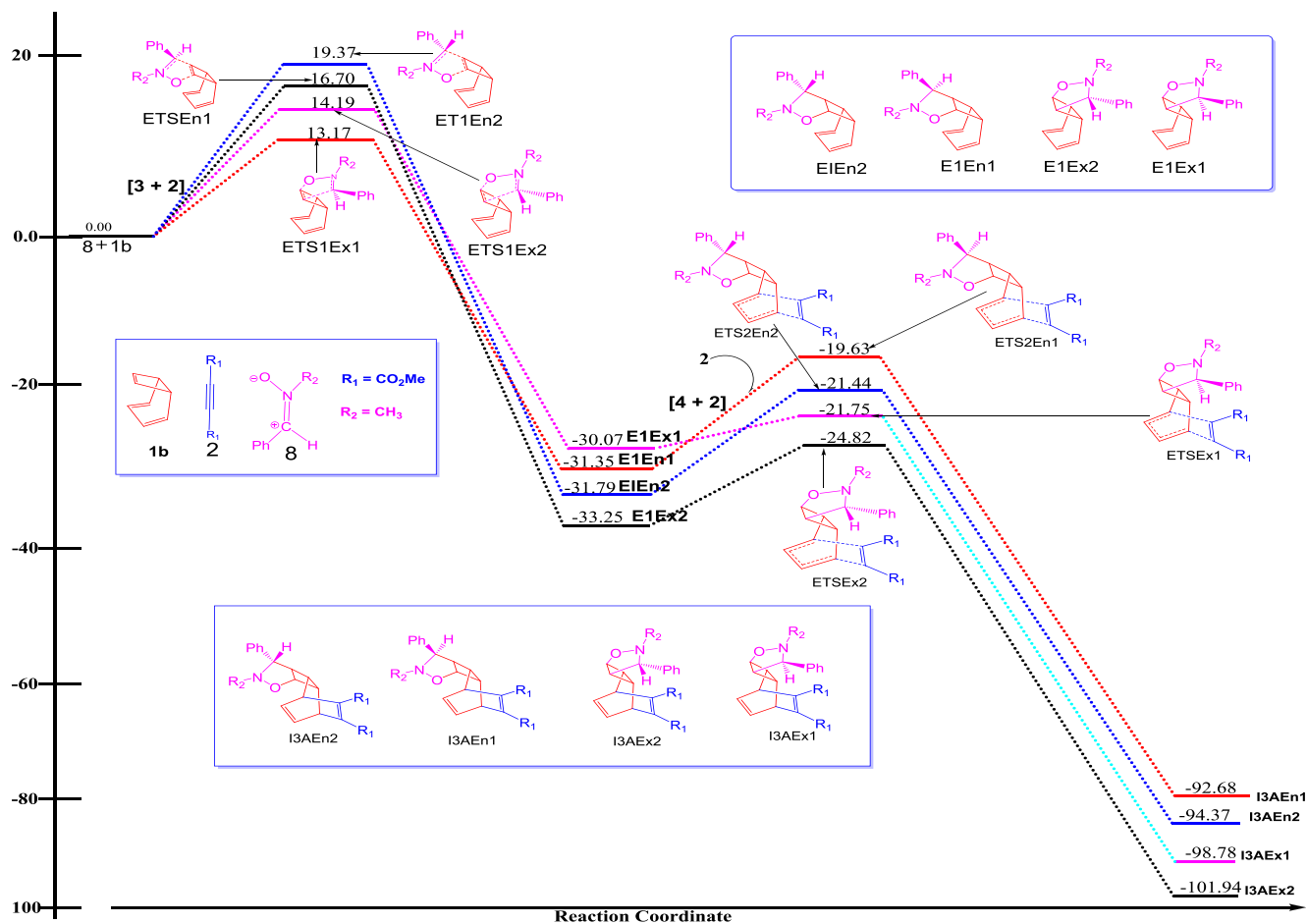


Fig. 9. Zero point energy corrected Gibbs free energy profile of the tandem [3 + 2] addition reaction of N-methyl-C-phenylnitron (**8a**) and COTE (**1b**) and follow up [4 + 2] addition of the adducts to dimethyl acetylenedicarboxylate (**2**) in benzene at the M06-2X/6-311G(d,p) level of theory.

bond > cyclobutene double bond contrary to the speculation by Bianchi et al. [17] that the substituted cyclohexadiene double bond is unreactive towards nitrones. In the case of the acyclic nitrones, the reactivity order is greatly influenced by the type of substituent on the nitrogen; however we found all the three double bonds to be reactive in all considered instances.

Finally, the mechanistic possibilities of [3 + 2]/[4 + 2] addition sequences involving the same reaction components in the case of cyclic and acyclic nitrones are explored extensively. The results are very encouraging, in most cases suggesting novel and convenient mechanistic routes for obtaining products of high selectivity with less energetic requirements. In some instances, new cycloadducts hitherto unreported are obtained. It is expected that this thorough study will further escalate the interest of synthetic chemists in the utilization of the tandem sequential cycloaddition reactions for the synthesis of relevant products and precursors considering the insights provided in this paper.

Competing interest

The authors declare that there is no conflict of interests whatsoever regarding the publication of this manuscript.

Acknowledgements

The authors are very grateful to the National Council for Tertiary Education, Republic of Ghana, for a research grant under the Teaching and Learning Innovation Fund (TALIF/KNUST/3/0008/2005), and to South Africa's Centre for High Performance Computing for access to additional computing resource.

Appendix A. Supplementary data

Supplementary data to this article can be found online at <https://doi.org/10.1016/j.jmgm.2019.06.019>.

References

- [1] S.E. Denmark, A. Thorarensen, Tandem [4+2]/[3+2] cycloadditions of nitroalkenes, *Chem. Rev.* 96 (1996) 137–166, <https://doi.org/10.1021/cr940277f>.
- [2] R.A. Bunce, Recent advances in the use of tandem reactions for organic synthesis, *Tetrahedron* 51 (1995) 13103–13159.
- [3] J.E. Sears, D.L. Boger, Tandem intramolecular diels-alder/1,3-dipolar cycloaddition cascade of 1,3,4-oxadiazoles: initial scope and applications, *Acc. Chem. Res.* 49 (2016) 241–251, <https://doi.org/10.1021/acs.accounts.5b00510>.
- [4] D.A. Margeti, P.A. Tro, M.R.B. Johnston, Tandem [4+2]/[3+2] cycloadditions of 1,3,4-oxadiazoles with alkenes, *Mini-Reviews Org. Chem.* 8 (2011) 49–65, <https://doi.org/10.2174/157019311793979981>.
- [5] S. Karlsson, H.-E. Högborg, Asymmetric 1,3-dipolar cycloadditions for the construction of enantiomerically pure heterocycles. A review, *Org. Prep. Proced. Int.* 33 (2001) 103–172, <https://doi.org/10.1080/00304940109356583>.
- [6] H. Pellissier, Stereocontrolled domino reactions, *Chem. Rev.* (2012) 442–524, <https://doi.org/10.1021/cr300271k>.
- [7] H. Pellissier, Recent developments in asymmetric organocatalytic domino reactions, *Adv. Synth. Catal.* 354 (2012) 237–294, <https://doi.org/10.1002/adsc.201100714>.
- [8] S.E. Denmark, R.Y. Baiazitov, Tandem double-intramolecular [4+2]/[3+2] cycloadditions of nitroalkenes. Studies toward a total synthesis of daphnilactone B: piperidine ring construction, *J. Org. Chem.* 71 (2006) 593–605, <https://doi.org/10.1021/jo052001l>.
- [9] S. Danishefsky, P.F. Schuda, T. Kitahara, S.J. Etheredge, The total synthesis of dl-vernolepin and dl-vernomenin, *J. Am. Chem. Soc.* 99 (1977) 6066–6075, <https://doi.org/10.1021/ja00460a038>.
- [10] J.E. Sears, T.J. Barker, D.L. Boger, Total synthesis of (–)-Vindoline and (+)-4-epi-vindoline based on a 1,3,4-oxadiazole tandem intramolecular [4 + 2]/[3 + 2] cycloaddition cascade initiated by an allene dienophile, *Org. Lett.* 17 (2015) 5460–5463, <https://doi.org/10.1021/acs.orglett.5b02818>.
- [11] J.D. Winkler, Tandem Diels–Alder cycloadditions in organic synthesis, *Chem. Rev.* 96 (1996) 167–176, <https://doi.org/10.1021/cr950029z>.
- [12] L.F. Fietze, Domino-reactions: the tandem-knoevenagel-hetero-diels-alder reaction and its application in natural product synthesis, *J. Heterocycl. Chem.* 27 (1990) 47–69, <https://doi.org/10.1002/jhet.5570270105>.
- [13] K.C. Nicolaou, T. Montagnon, S.A. Snyder, Tandem reactions, cascade sequences, and biomimetic strategies in total synthesis, *Chem. Commun.* 0 (2003) 551–564, <https://doi.org/10.1039/b209440c>.
- [14] C. Chapman, C. Frost, Tandem and domino catalytic strategies for enantioselective synthesis, *Synthesis (Stuttg.)* (2007) 1–21, <https://doi.org/10.1055/s-2006-950379>, 2007.
- [15] S.E. Denmark, R.Y. Baiazitov, S.T. Nguyen, Tandem double intramolecular [4+2]/[3+2] cycloadditions of nitroalkenes: construction of the pentacyclic core structure of daphnilactone B, *Tetrahedron* 65 (2009) 6535–6548, <https://doi.org/10.1016/j.tet.2009.05.060>.
- [16] G. Bianchi, A. Gamba, R. Gandolfi, Cycloaddition reactions of nitrones to cyclooctatetraene and its derivatives, *Tetrahedron* 28 (1972) 1601–1609, [https://doi.org/10.1016/0040-4020\(72\)88042-6](https://doi.org/10.1016/0040-4020(72)88042-6).
- [17] G. Bianchi, R. Gandolfi, P. Grünanger, Cycloaddition of nitrile imines to cyclooctatetraene, *Tetrahedron* 29 (1973) 2405–2410, [https://doi.org/10.1016/S0040-4020\(01\)93370-8](https://doi.org/10.1016/S0040-4020(01)93370-8).
- [18] S.E. Denmark, D.S. Middleton, Mode, Efficient and highly selective synthesis of azapropellanes, *J. Org. Chem.* 3263 (1998) 1604–1618.
- [19] U. Chiacchio, A. Corsaro, J. Mates, P. Merino, A. Piperno, A. Rescifina, G. Romeo, R. Romeo, T. Tejero, Isoxazolidine analogues of pseudouridine: a new class of modified nucleosides, *Tetrahedron* 59 (2003) 4733–4738, [https://doi.org/10.1016/S0040-4020\(03\)00689-6](https://doi.org/10.1016/S0040-4020(03)00689-6).
- [20] Heterocyclic Substituted Isoxazolidines and Their Use as Fungicides, 2000, <https://patents.google.com/patent/US6313147B1/en>.
- [21] S.A. Ali, M.T. Saeed, S.U. Rahman, The isoxazolidines: a new class of corrosion inhibitors of mild steel in acidic medium, *Corros. Sci.* 45 (2003) 253–266, [https://doi.org/10.1016/S0010-938X\(02\)00099-9](https://doi.org/10.1016/S0010-938X(02)00099-9).
- [22] N.A. LeBel, M.E. Post, J.J. Whang, The addition of nitrones to olefins. Fused bicyclic isoxazolidines, *J. Am. Chem. Soc.* 86 (1964) 3759–3767, <https://doi.org/10.1021/ja01072a031>.
- [23] C. Belzecki, I. Panfil, Cycloaddition of chiral nitrones. Asymmetric synthesis of isoxazolidines, *J. Org. Chem.* 44 (1979) 1212–1218, <https://doi.org/10.1021/jo01322a005>.
- [24] P. Righi, E. Marotta, A. Landuzzi, G. Rosini, Silicon-tethered 1,3-dipolar cycloaddition of 4-hydroxy-2-isoxazoline 2-oxides, *J. Am. Chem. Soc.* 118 (1996) 9446–9447, <https://doi.org/10.1021/ja961816w>.
- [25] M. Frederickson, Optically active isoxazolidines via asymmetric cycloaddition reactions of nitrones with alkenes: applications in organic synthesis, *Tetrahedron* 53 (1997) 403–425, [https://doi.org/10.1016/S0040-4020\(96\)01095-2](https://doi.org/10.1016/S0040-4020(96)01095-2).
- [26] N. Jegham, A. Bahi, N. El Guesmi, Y. Kacem, B. Ben Hassine, Regio- and stereoselective synthesis of new spiro-isoxazolidines via 1,3-dipolar cycloaddition, *Arab. J. Chem.* 10 (2017) S3889–S3894, <https://doi.org/10.1016/j.arabj.2014.05.028>.
- [27] R.L. Lalonde, Z.J. Wang, M. Mba, A.D. Lackner, F.D. Toste, Gold(I)-Catalyzed enantioselective synthesis of pyrazolidines, isoxazolidines, and tetrahydrooxazines, *Angew. Chem.* 122 (2010) 608–611, <https://doi.org/10.1002/ange.200905000>.
- [28] K. Rück-Braun, T.H.E. Freysoldt, F. Wierschem, 1,3-Dipolar cycloaddition on solid supports: nitron approach towards isoxazolidines and isoxazolines and subsequent transformations, *Chem. Soc. Rev.* 34 (2005) ss, <https://doi.org/10.1039/b311200b>.
- [29] L. Domingo, Theoretical studies on domino cycloaddition reactions, *Mini-Reviews Org. Chem.* 2 (2005) 47–57, <https://doi.org/10.2174/1570193052774063>.
- [30] Wavefunction, Spartan 14^v.1.1.8, Wavefunction, 2014.
- [31] M.J. Frisch, G.W. Trucks, H.B. Schlegel, G.E. Scuseria, M.A. Robb, J.R. Cheeseman, G. Scalmani, V. Barone, B. Mennucci, G.A. Petersson, H. Nakatsuji, M. Caricato, X. Li, H.P. Hratchian, A.F. Izmaylov, J. Bloino, G. Zheng, J.L. Sonnenberg, M. Hada, M. Ehara, K. Toyota, R. Fukuda, J. Hasegawa, M. Ishida, T. Nakajima, Y. Honda, O. Kitao, H. Nakai, T. Vreven, J.A. Montgomery, J.E. Peralta, F. Ogliaro, M. Bearpark, J.J. Heyd, E. Brothers, K.N. Kudin, V.N. Staroverov, R. Kobayashi, J. Normand, K. Raghavachari, A. Rendell, J.C. Burant, S.S. Iyengar, J. Tomasi, M. Cossi, N. Rega, J.M. Millam, M. Klene, J.E. Knox, J.B. Cross, V. Bakken, C. Adamo, J. Jaramillo, R. Gomperts, R.E. Stratmann, O. Yazyev, A.J. Austin, R. Cammi, C. Pomelli, J.W. Ochterski, R.L. Martin, K. Morokuma, V.G. Zakrzewski, G.A. Voth, P. Salvador, J.J. Dannenberg, S. Dapprich, A.D. Daniels, Ö. Farkas, J.B. Foresman, J.V. Ortiz, J. Cioslowski, D.J. Fox, Gaussian 09, Revision B. 01, Gaussian Inc., Wallingford, CT, 2009 6492.
- [32] Y. Zhao, D.G. Truhlar, Density functionals with broad applicability in chemistry, *Acc. Chem. Res.* 41 (2008) 157–167, <https://doi.org/10.1021/ar700111a>.
- [33] S.N. Pieniazek, K.N. Houk, The origin of the halogen effect on reactivity and reversibility of diels–alder cycloadditions involving furan, *Angew. Chem. Int. Ed.* 45 (2006) 1442–1445, <https://doi.org/10.1002/anie.200502677>.
- [34] R.S. Paton, J.L. Mackey, W.H. Kim, J.H. Lee, S.J. Danishefsky, K.N. Houk, Origins of stereoselectivity in the *trans* Diels–Alder paradigm, *J. Am. Chem. Soc.* 132 (2010) 9335–9340, <https://doi.org/10.1021/ja1009162>.
- [35] R.S. Paton, S.E. Steinhardt, C.D. Vanderwal, K.N. Houk, Unraveling the mechanism of cascade reactions of zinc aldehydes, *J. Am. Chem. Soc.* 133 (2011) 3895–3905, <https://doi.org/10.1021/ja107988b>.
- [36] S.E. Wheeler, A. Moran, S.N. Pieniazek, K.N. Houk, Accurate reaction enthalpies and sources of error in DFT thermochemistry for Aldol, Mannich, and α -aminoxylation reactions, *J. Phys. Chem. A* 113 (2009) 10376–10384, <https://doi.org/10.1021/jp9058565>.
- [37] J. Tomasi, B. Mennucci, R. Cammi, Quantum mechanical continuum solvation

- models, Chem. Rev. 105 (2005) 2999–3094, <https://doi.org/10.1021/CR9904009>.
- [38] M. Clark, R.D. Cramer, N. Van Opdenbosch, Validation of the general purpose tripos 5.2 force field, J. Comput. Chem. 10 (1989) 982–1012, <https://doi.org/10.1002/jcc.540100804>.
- [39] E. Opoku, R. Tia, E. Adei, [3 + 2] versus [2 + 2] Addition : a density functional theory study on the mechanistic aspects of transition metal-assisted formation of 1, 2-dinitrosoalkanes, J. Chem. 2016 (2016) 10, <https://doi.org/10.1155/2016/4538696>.
- [40] E. Opoku, R. Tia, E. Adei, Computational studies on [4+2]/[3+2] tandem sequential cycloaddition reactions of functionalized acetylenes with cyclopentadiene and diazoalkane for the formation of norbornene pyrazolines, J. Mol. Model. 25 (2019) 168, <https://doi.org/10.1007/s00894-019-4056-x>.
- [41] E. Opoku, R. Tia, E. Adei, DFT mechanistic study on tandem sequential [4 + 2]/[3 + 2] addition reaction of cyclooctatetraene with functionalized acetylenes and nitrile imines, J. Phys. Org. Chem. (2019), e3992, <https://doi.org/10.1002/poc.3992>.
- [42] E. Vogel, H. Kiefer, W. Roth, Bicyclo[4,2,0]octa-2,4,7-triene, Angew. Chem. Int. Ed. Engl. 3 (1964) 442–443, <https://doi.org/10.1002/anie.196404422>.
- [43] R. Sustmann, A simple model for substituent effects in cycloaddition reactions. I. 1,3-dipolar cycloadditions, Tetrahedron Lett. 12 (1971) 2717–2720, [https://doi.org/10.1016/S0040-4039\(01\)96961-8](https://doi.org/10.1016/S0040-4039(01)96961-8).
- [44] K.N. Houk, Frontier molecular orbital theory of cycloaddition reactions, Acc. Chem. Res. 8 (1975) 361–369, <https://doi.org/10.1021/ar50095a001>.